APPENDIX

The value of the critical noise intensity $S_{cr} = \langle f^2 \rangle_{cr}$ and values of the parameter $G = [\langle \tilde{n} \rangle_\eta^2 / \eta^2]_{S=S_{cr}}$, which characterizes satisfaction of the criterion for weak fluctuations, for media of various dimensionalities ($d = 1, 2, 3$) for various relations between r_{diff}, l, and r_0:

I. $d=1$. a) $r_{diff} \gg r_0 \gg l$ $(\alpha \ll Dk_0^2 \ll \gamma)$,

$$S_{cr}^{1/2} = \alpha(r_{diff}/l), \quad G = r_0/r_{diff} \ll 1.$$

b) $r_{diff} \gg l \gg r_0$ $(\alpha \ll \gamma \ll Dk_0^2)$,

$$S_{cr}^{1/2} = \alpha(r_{diff}/r_0^{1/2} l^{1/2}), \quad G = l/r_{diff} \ll 1.$$

c) $r_0 \gg r_{diff}, l$ $(Dk_0^2 \ll \alpha, \gamma)$, $G \gtrsim 1$.
d) $l \gg r_{diff}, r_0$ $(\gamma \ll \alpha, Dk_0^2)$, $G \gtrsim 1$.

II. $d=2$. a) $r_{diff} \gg r_0 \gg l$ $(\alpha \ll Dk_0^2 \ll \gamma)$,

$$S_{cr}^{1/2} = \alpha r_{diff}/l, \quad G = (r_0/r_{diff})^2 \ln(2r_{diff}/r_0) \ll 1.$$

b) $r_{diff} \gg l \gg r_0$ $(\alpha \ll \gamma \ll Dk_0^2)$,

$$S_{cr}^{1/2} = \frac{\alpha r_{diff}}{r_0} \left(\ln \frac{2l}{r_0} \right)^{-1/2}, \quad G = \left(\frac{l}{r_{diff}} \right)^2 \ln \frac{r_{diff}}{l} \Big/ \ln \frac{2l}{r_0} \ll 1.$$

c) $r_0 \gg r_{diff}, l$ $(Dk_0^2 \ll \gamma, \alpha)$, $G \gtrsim 1$.
d) $l \gg r_{diff}, r_0$ $(\gamma \ll \alpha, Dk_0^2)$, $G \gtrsim 1$.

III. $d=3$. a) $r_{diff} \gg r_0 \gg l$ $(\alpha \ll Dk_0^2 \ll \gamma)$,

$$S_{cr}^{1/2} = \alpha r_{diff}/l, \quad G = (r_0/r_{diff})^2 \ll 1.$$

b) $r_{diff} \gg l \gg r_0$ $(\alpha \ll \gamma \ll Dk_0^2)$

$$S_{cr}^{1/2} = \alpha r_{diff}/r_0, \quad G = 2r_0 l/r_{diff}^2 \ll 1.$$

c) $r_0 \gg r_{diff}, l$ $(Dk_0^2 \ll \alpha, \gamma)$, $G \gtrsim 1$.
d) $l \gg r_0 \gg r_{diff}$ $(\gamma \ll Dk_0^2 \ll \alpha)$, $G \gtrsim 1$.
e) $l \gg r_{diff} \gg r_0$ $(\gamma \ll \alpha \ll Dk_0^2)$,

$$S_{cr}^{1/2} = \alpha r_{diff}/r_0, \quad G = r_0/r_{diff} \ll 1.$$

[1] The best known example of such an effect is parametric excitation of a classical oscillator (see Ref. 1).
[2] This procedure is exactly equivalent to the self-consistent field approximation in the theory of equilibrium phase transition.

[1] V. I. Klyatskin, Statisticheskoe opisanie dinamicheskikh sistem s fluktuiruyushimi parametrami (Statistical Description of Dynamical Systems with Flucturating Parameters), Nauka, 1975, Chap. 6.
[2] D. A. Frank-Kamentskii, Diffuziya i teploperadacha v khimicheskoi kinetike (Diffusion and Heat Transfer in Chemical Kinetics), Nauka, 1967 (translation, Plenum Press, 1969).
[3] L. D. Landau and E. M. Lifshitz, Kvantovaya mekhanika. Nerelyativistskaya teoriya (Quantum Mechanics. Nonrelativistic Theory), Nauka, 1974, 41 (translation, Pergamon Press, 1977).
[4] I. M. Lifshitz, S. A. Gredeskul, and L. A. Pastur, Fiz. Nizk. Temp. 2, 1093 (1976) [Sov. J. Low Temp. Phys. 2, 533 (1976)].
[5] A. S. Mikhailov, Dokl. Akad. Nauk SSSR 243, 786 (1978) [Doklady Biophysics 243, 191 (1978)]; Phys. Lett. 73A, 143 (1979).

Translated by W. F. Brown, Jr.

Transmission of sound across a boundary between liquid helium and a metal

K. N. Zinov'eva

Institute of Physics Problems, Academy of Sciences of the USSR, Moscow

A description of the experimental procedure is followed by a report of the results of investigations of the angular dependence of the transmission of a plane monochromatic acoustic wave incident from liquid ^{4}He on the surfaces of tungsten and gold. The energy of 10–30 MHz sound was deduced from measurements of the Kapitza temperature jump at the liquid helium–metal boundary at temperatures 0.1–0.4 °K. A resonance energy transmission peak was observed experimentally outside the critical cone when sound was incident at the Rayleigh angle. This effect was considered using the generalized acoustic theory and the theory of Andreev. The contribution of the energy associated with the Rayleigh peak was approximately equal to the energy in the subcritical angle. A comparison was made of the attenuation of surface waves on tungsten with the known theoretical and experimental coefficients representing the bulk absorption of sound due to an electron mechanism.

PACS numbers: 68.25. + j, 43.35.Lq, 43.35.Pt

INTRODUCTION

The present author reported earlier[1] the observations of resonance absorption of sound by the surface of a metal. The effect was predicted theoretically by Andreev[2] and it was due to dissipation of the energy of a Rayleigh wave excited in the metal by the incident sound. The present paper describes an investigation of the angular and frequency dependences of the transmission coefficient $w(\theta, \omega)$ of the acoustic energy crossing the boundary between liquid ^{4}He and a metal.

The idea of measuring $w(\theta, \omega)$ has been put forward in several laboratories some years ago after numerous attempts to explain fully the Kapitza temperature jump[3] which appears at an interface when heat is transferred from a solid body to liquid helium. Kapitza showed that this temperature jump ΔT is proportional to the heat flux density $\dot{Q}/S$ and to the thermal resistance of the boundary (contact resistance) R_c, which varies with temperature as T^{-3}.

A theoretical explanation of the Kapitza jump was giv-

en by Khalatnikov[4,5] and Little.[6] Khalatnikov showed the process of heat exchange between a solid body and liquid helium involves absorption and emission of phonons by the surface of the solid. Two factors impede the establishment of an equilibrium. Firstly, the phonon transmission coefficient is low (~10^{-3}) because of the considerable difference between the acoustic impedances of liquids and solids.[5,7] Secondly, the majority of phonons incident from helium on the interface at an angle $\theta > \theta_2$ $= \sin^{-1}(c/c_t)$, where c is the velocity of sound in the liquid and c_t is the velocity of transverse sound in the solid, is totally reflected. For most solids immersed in liquid helium the critical angle is $\theta_2 \lesssim 10°$. For these reasons the energy incident on the interface is almost totally reflected and this results in overheating of one medium relative to the other.

Heat exchange may improve somewhat when a Rayleigh wave is excited on the surface of the solid by the incident phonons. However, this wave can transfer its energy to the solid only in the case of a strong coupling with bulk or other excitations in the solid. No direct experimental proof has yet been obtained of an additional transmission of the acoustic energy at low temperatures due to the absorption of Rayleigh waves. However, it has been firmly established that a considerable improvement in the exchange of heat results from imperfections of the surface of a solid,[8] which may be due to a strong attenuation of Rayleigh waves in a thin surface layer.[9]

The flux of heat from liquid helium at a temperature T to a solid[5,9] can be written in the form

$$\dot{Q}_{l \to s} = \frac{\hbar}{(2\pi c)^2} \int_0^\infty n\left(\frac{\hbar\omega}{T}\right) \omega^3 \, d\omega \int_0^{\pi/2} w(\theta, \omega) \cos\theta \sin\theta \, d\theta. \quad (1)$$

Here, n is the Planck distribution function and $w(\theta, \omega)$ is the transmission coefficient of a phonon of frequency ω incident from liquid helium on a solid at an angle θ. The flux of heat from a solid whose temperature is T_1 to liquid helium can be described by a similar expression if allowance is made in the integral (1) for all types of wave excited in the solid. The net heat flux for $T_1 \neq T$ is equal to the difference between the energy fluxes directed from the solid to the liquid and from the liquid to the solid. Hence, the value as well as the frequency and angular dependences of the transmission coefficient $w(\theta, \omega)$ play an important role in the exchange of heat between helium and solids and, consequently, in the Kapitza resistance.

The transmission coefficient outside the critical angle, when surface Rayleigh waves may be excited in a solid by the incident phonons, is of particular interest. In calculating the flow of heat across a boundary, Khalatnikov assumed that Rayleigh waves are in equilibrium with the solid. However, the actual mechanisms of the absorption of the surface-wave energy by the solid was not considered by Khalatnikov.[4,5]

Little[10] and Andreev[2] pointed out that in the case of metals one of the relevant mechanisms can be the interaction of phonons with conduction electrons. Andreev showed that if allowance is made for the absorption of sound by conduction electrons, the transmission coef-

ficient of sound incident at the Rayleigh angle should have a sharp peak of height of the order of unity and width of the order of $\rho c^2/D c_t^2$, where ρ and D are the densities of helium and of the metal in question. The Rayleigh angle of incidence θ_R lies within the range of total internal reflection close to θ_2 and can be found from

$$\sin\theta_R = c/c_R = c/\xi c_t, \quad (2)$$

where c_R is the velocity of Rayleigh waves on a free metal surface and ξ lies within the range $0.87 < \xi < 0.96$ (Ref. 11).

Somewhat later several authors[12-15] have described the phenomenon of transmission of thermal phonons across an interface between two media at low temperatures by a phenomenological generalized acoustic theory,[16,17] which allows for the bulk absorption of sound in a solid. The theoretical behavior of $w(\theta)$ in the vicinity of the Rayleigh angle was found to be similar to that predicted by Andreev.

The first experimental investigation of the angular distribution of the emission and absorption of thermal phonons by the surface of an NaF crystal immersed in liquid helium was carried out by a pulse method.[14,15] It was found that only a small proportion of the energy was emitted in the critical cone, whereas most of the energy (85%) passed outside the cone in the form of wide wings. This behavior was described satisfactorily by the generalized acoustic theory, but because of the large angular dimensions of the emitter and receiver (8° and 3°), it was not possible to study the structure of $w(\theta)$ in detail.

We shall describe the measurement method and the results obtained for the interface between liquid ^{4}He and tungsten or gold. We shall report a calculation of theoretical dependences carried out on a computer using the formulas of the generalized acoustic theory. We shall compare the experimental results with this theory and that of Andreev.

1. THEORY

The energy transmission coefficient $w(\theta, \omega) = I_2/I_0$, of a plane acoustic wave of frequency ω incident from a liquid on the surface of a solid at an angle θ and the reflection coefficient $v(\theta, \omega) = I_1/I_0$ are related by $w = 1 - v$, where i_0, I_1, and I_2 are the intensities (energies) of the incident, reflected, and transmitted waves.

The transmitted acoustic energy I_2 consists of the energies of all types of vibrations of the solid and, if sound is absorbed in the solid, it is converted into heat. In view of the large difference between the acoustic impedances of liquid helium and a solid body, the reflection coefficient is close to unity if we ignore the acoustic waves which emerge from the solid and are transmitted back to the liquid. Thus, with a high degree of precision, the transmission coefficient is equal to the fraction of the incident energy absorbed by the solid. Since the time for relaxation of acoustic into thermal phonons in a metal at $T \sim 0.1\,°$K ($\tau \lesssim 10^{-6}$ sec, Ref. 18) is much shorter than the time needed to establish a

thermal equilibrium between the liquid and solid ($\tau \sim 10^{-2}$ sec), the temperature of the solid may rise by an amount ΔT corresponding to the Kapitza jump.

Under steady-state conditions during continuous emission of sound the energy flux of acoustic phonons from a liquid to a solid is compensated by the return flux of thermal phonons from the solid to the liquid: $\dot{Q}_{a.ph}^{l-s} = \dot{Q}_{t.ph}^{s-l}$ or

$$wN\sigma_0 \cos\theta = \frac{S\Delta T}{R_c},$$

so that

$$\Delta T = \frac{N\sigma_0 \cos\theta\, wR_c}{S}. \tag{3}$$

Here, N is the density of the acoustic energy flux on the surface of the solid; $\sigma_0 \cos\theta$ is the area of the sample on which the sound is incident (this area is taken to be normal to the acoustic flux); S is the total area of the sample.

It follows from Eq. (3) that overheating of the sample by ΔT is proportional to the energy of the acoustic flux, (divided by the total area of the sample $N\sigma_0 \cos\theta/S$), to the acoustic transmission coefficient w, and to the Kapitza contact resistance R_c. If the dependence $\Delta T(\theta)$ is determined at a constant liquid temperature T for various values of ω, it is possible to find experimentally

$$w(\theta,\omega) = \frac{S\Delta T}{R_c N\sigma_0 \cos\theta}$$

or

$$\alpha(\theta,\omega) = w\cos\theta = \frac{S\Delta T}{R_c N\sigma_0}. \tag{4}$$

Only the relative value of $\alpha(\theta, \omega)$ was determined experimentally. The absolute value could be found either by normalizing α through equating the experimental value to the theoretical one for zero angle or by determining independently (using some other method) the energy incident on a sample and absorbed by it.

2. APPARATUS

The experiments involved determination of the acoustically induced increase in the temperature of a sample as a function of the angle of incidence of the sound. A piezoelectric quartz transducer emitting a plane monochromatic acoustic wave was placed in a chamber with liquid helium. A sample of the investigated metal was placed at a distance of ~1 cm from the sound source. Rotation of this sample made it possible to vary the angle of incidence θ found with a capacitance probe. Two identical semiconductor thermometers, one of which was placed in liquid helium and the other was bonded to the sample, made it possible to determine the absolute temperature of the liquid and the metal, as well as the difference between these temperatures (for details see Figs. 1–3).

General setup

The measurements were carried out in a ^{3}He–^{4}He solution cryostat with ^{3}He circulating at a rate of 10^{-6} to 2×10^{-4} mole/sec. The cryostat had one monolithic and five sintered copper heat exchangers. In the absence of
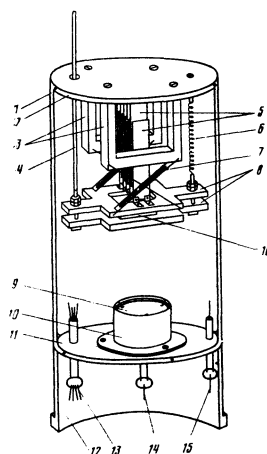

FIG. 1. Measuring cell: 1) metal insert; 2), 11) supporting disks; 3) supports; 4) rod; 5) variable-capacitor plates; 6) spring; 7) four flat springs; 8) double frame; 9) piezoelectric quartz transducer; 10) transducer holder; 12) cylindrical can; 13)–15) electrical leads; 16) sample.

a load in the solution chamber, such circulation produced temperatures of $(10-15)\times10^{-3}$ °K. A measuring chamber of ~50 cm^3 volume and the solution chamber were made from the same copper block and were separated by a wall 4 mm thick. Condensation of ^{4}He took place in the measuring chamber along a German silver capillary 0.2 mm in diameter and 1.5 m long. Heat transfer along the ^{4}He film was avoided by ensuring a good thermal contact between the capillary, on the one hand, and the evaporation chamber and heat exchangers, on the other.

The temperature of the liquid in the measuring chamber was measured with carbon and germanium thermometers, which were first calibrated using the magnetic susceptibility of cerium-magnesium nitrate and the vapor pressure of ^{3}He. The constancy of the calibration was checked with a ^{3}He condensation thermometer in the measuring chamber. The thermometer at-
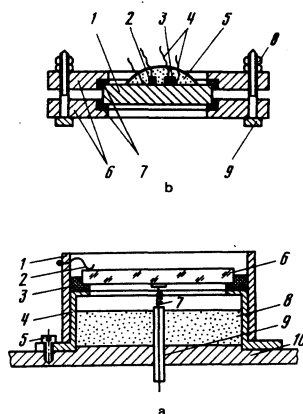

FIG. 2. Sound source and sample. a) Piezoelectric quartz transducer; 1) bronze cylinder; 2) three contact springs; 3) paper spacer; 4) stage; 5) screw; 6) piezoelectric quartz plate; 7) contact spring; 8) sound absorber; 9) insulator; 10) support disk. b) Sample holder: 1) sample; 2), 3) thermometers; 4) electrical leads; 5) epoxy resin; 6) double frame; 7) Textolite spacers; 8) nuts; 9) screw.
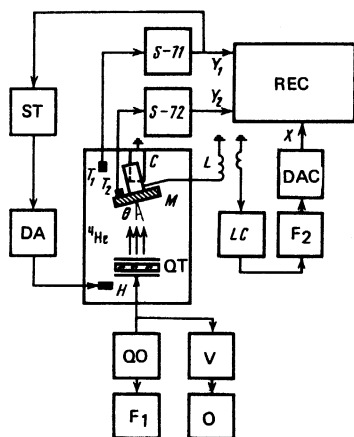
FIG. 3. Block diagram of the apparatus: QT is a piezoelectric quartz transducer, M is a metal sample, θ is the angle of incidence of sound, C is a variable capacitor, T_1 and T_2 are thermometers in the liquid and on the sample, H is a heater, QO is an oscillator supplying the quartz transducer, F_1 is a frequency meter, V is a voltmeter, O is an oscilloscope, ST is a stabilizer of the temperature in the ^{4}He bath, S-71 and S-72 are ac bridges, L is an inductor, LC is an oscillator for the angle-of-rotation tensory, F_2 is a meter for measuring the frequency of the LC oscillator, DAC is a digital–analog converter, REC is an X-Y two-pen recorder, and DA is a digital ammeter.

tached to the sample was calibrated against the thermometer in the liquid after each run.

Measuring chamber

The measuring chamber was an inverted can 4 cm in diameter and 5 cm high. The bottom of the can was also the bottom of the solution bath. The light metal framework 1 (Fig. 1) consisted of two parallel disks 2 and 11 linked by thin vertical rods. The upper disk carried the sample, which could be moved, and the lower disk carried the transducer, which had a fixed position. The lower disk also formed the bottom of an inverted small can 12. After alignment, the lower edge of the can 12 was soldered hermetically to the measuring chamber.

The sample 16 was clamped in a double metal frame 8, suspended by four flat springs 7 to supports 3 attached to the upper disk 2. The frame together with the sample were rotated by a rod 4 and a return spring 6, which set the initial angle $\theta \sim 20°$ between the sample and the quartz transducer. The flat springs 7 made it possible to rotate the sample in one plane. The upper part of the frame 8 carried a set of adjustable parallel plates 5 forming a variable capacitor of capacitance C. Fixed plates were attached to the disk 2. The change in the capacitance was proportional to the angle θ. The angle $\theta = 0$ corresponded to the maximum capacitance.

The rod 4 made of michrome wire 0.3 mm in diameter passed through the cover of the measuring chamber via a bellows and projected into the vacuum jacket of the cryostat. When the initial angle θ was set, the wire was sealed hermetically in the bellows. The rod was moved by a second bellows soldered to the upper cover of the vacuum jacket and connected to the lower bellows

by a bakelite rod. Condensation of helium in the upper bellows and continuous variation of its pressure made it possible to vary the angle θ from −20 to +20° at a constant rate and this rate could be altered within a wide range.

The quartz transducer 9 was placed in a special holder 10 and mounted on the lower disk 11 in such a way that the centers of the sample and quartz transducer were on the same vertical line. Electrical leads made of a superconducting wire (tinplated constantan) passed into the measuring chamber via platinum–glass joints 13–15.

Sound source

Sound of 10, 20, and 30 MHz frequencies was generated by circular (15 mm in diameter) and rectangular (10×11 mm) X-cut quartz plates. Special attention was paid to the homogeneity of acoustic radiation. The characteristics of these quartz transducers were investigated by electronic and optical methods. The quartz plates with the best frequency characteristics at room and helium temperatures were selected. At room temperature the dark-field method was used to study the radial distribution of the intensity of the acoustic beam and its angular divergence in water and toluene. This was done by photographing the traveling and standing waves formed as a result of interaction between the direct and reflected (at a small angle) waves.

When the acoustic radiation was homogeneous, the traveling-wave image (which appeared as a dome because of the attenuation in the liquid) was unaffected by rotation of the quartz plate. The interference pattern of the standing waves was a system of parallel fringes. Deviation from parallelism indicated divergence of the acoustic beam. In the case of the better quartz plates operating at 10 MHz the divergence of the beam in beam and toluene at room temperature was (within the limits of the experimental error) equal to the diffraction limit: $\lambda/d = 36'$.

It was established that the method of clamping the quartz plate had an important influence on its characteristics. When the mechanical contact between the quartz plate and a holder was minimal and the plate emitted sound freely in the liquid, the efficiency was maximal and there were only slight distortions in the frequency characteristic in liquid helium. A quartz transducer and its mounting are shown in Fig. 2(a). A quartz plate 6 with gold films evaporated on both sides lay freely on a circular polished table 4 made of stainless steel and provided with a central aperture of the same shape as the plate but of slightly smaller dimensions. The plate was isolated from the table by a ring-shaped paper spacer 3. Electrical contacts with the top and bottom surfaces of the plate were made by light phosphor-bronze springs 2 and 7, whose diameter was 70 μ. The upper springs were soldered to a thin bronze cylinder 1 fitted onto the table from above.

The quartz plate emitted in both directions. The acoustic radiation directed downward was absorbed by a sintered copper filter 8.

Samples

Our measurements were made on two samples: a polycrystalline gold piece and a tungsten single crystal; the ratio of the electrical resistances at room and helium temperatures was $R_{300}/R_{4.2} = 36\,000$ for gold and $64\,000$ for tungsten. The gold sample was a parallelepiped of $13 \times 10 \times 1.9$ mm dimensions and it was shaped by rolling followed by flattening in a press between polished quartz plates. The tungsten single crystal [1 in Fig. 2(b)] was a circular disk 8.6 mm in diameter and 1.5 mm thick. The normal to the frontal electropolished disk surface made angles of 23° and 30° with the [100] and [101] axes. The surface quality was monitored with a Linnik interferometer and it was found that the surface roughness and deviations from a planar surface in the case of gold did not exceed 0.5 μ, whereas in the case of tungsten they were 0.3 μ.

The carbon and germanium thermometers were soldered to the gold sample so as to form a single contact with thin strips ($d \sim 0.2$ mm) separated from the edge of the sample by spark machining. In the case of tungsten the corresponding thermometers 2 and 3 [Fig. 2(b)] were bonded to the rear surface of the single crystal by an electrically conducting adhesive. The direct contact of these thermometers with liquid helium was avoided by coating them with an epoxy resin mixed with a quartz powder 5. A bakelite spacer 7 insulated the samples from the contact with the frame 6.

Thermometers

The energy absorbed in the sample was measured with semiconductor resistance thermometers, which were in good thermal contact with the sample. Since the contact thermal resistance between two solids was known to be much less than the thermal resistance between a solid body and liquid helium, the thermometer and the sample were in thermal equilibrium with one another.

We used carbon and germanium thermometers with identical characteristics, whose resistances were nominally between 10^3 and $10^6 \ \Omega$ at $T < 1$ °K and whose sensitivity ranged from 10^{-4} to 10^{-7} °K/Ω. The temperature dependence of the electrical conductivity was either exponential or (sometimes) in the form of a power law. Carbon thermometers[19] were disks (3 mm in diameter and 1 mm thick), whose end surfaces carried electrolytic copper contacts. Germanium thermometers were made of originally pure single-crystal germanium which was subjected to subsequent neutron doping. They were cubes of $1 \times 1 \times 1$ mm dimensions with alloyed indium contacts.[20] The temperature of liquid helium was measured using thermometers made of the same material (and taken from the same batch) as the thermometer attached to the sample.

The thermometer resistances were measured with ac bridges at 237 Hz at voltages 6–60 μV across the thermometers corresponding to dissipation of 10^{-14}–10^{-12} W. The absolute temperatures of the liquid and metal were determined to within 10^{-3} °K, and the difference between these temperatures was found to within 10^{-6} °K. The rise of the thermometer temperature because of the flow of the measuring current did not exceed 5×10^{-7} °K.

Angle measurements

A capacitor with $C = 10$–20 pF and a coil with L = 450 μH (number of turns $n_1 = 400$), placed inside the solution cryostat, formed an oscillatory circuit resonant at 1.3–1.7 MHz.

A secondary winding ($n_2 = 2$–3 turns) wound on the induction coil L (Fig. 3) was connected by a coaxial cable to a noninverting input of a broadband amplifier with positive feedback. The amplifier was mounted on the cryostat cover and formed together with the circuit an LC oscillator.[1] When the self-excitation conditions were satisfied, the circuit generated spontaneous oscillations at the resonance frequency. The weak coupling between the oscillatory circuit and the amplifier ensured that the influence of the capacitance of the connecting cable on the oscillator parameters was only slight and that the frequency of oscillations was governed only by the capacitance C when the inductance was constant.

The frequency of the LC oscillator was measured with a frequency meter to within 1 Hz, so that the sensitivity in the determination of the rotation angle was of the order of 1″. The error in the absolute value of the angle amounted to ~10%, since it was governed (because of the geometry of the system) by the precision of the calibration carried out at room temperature.

Temperature stabilization

The very first experiments showed that the temperature of liquid helium in the measuring chamber did not remain constant. In addition to a temperature drift, rotation of the sample always resulted in a monotonic rise of the helium temperature by 10^{-4}–10^{-2} °K, depending on the rate of motion of the frame. There were also random temperature fluctuations of the same order due to a variety of reasons, principal among which were shocks and vibrations of the springs in the rotation system, and the vibrations of the solution cryostat itself.

After the first observations on gold, which showed that the acoustically induced increase in the temperature of the sample did not exceed 1×10^3 °K, it was found that the temperature of the liquid in the measuring chamber had to be stabilized. This was done with a stabilization system controlled by the signal and its two derivatives.[21]

3. EXPERIMENT

Pumping of helium vapor from the outer bath cooled the system to ~1.3 °K, when condensation of ^{4}He took place in the measuring chamber. Then, the condensation line was shut off by a valve in the cover throughout the rest of the experiment. Next, the spontaneously operating solution cryostat was activated.

When the temperature fell to $T \sim 0.1$ °K, the quartz transducer (Fig. 3) was subjected to an alternating voltage from a quartz oscillator QO. The ^{4}He temperature

1000   Sov. Phys. JETP 52(5), Nov. 1980

K. N. Zinov'eva   1000

then rose somewhat. When the oscillator was tuned to the resonance frequency of the quartz transducer, the amplitude of the voltage across the transducer was kept constant as monitored by voltmeter V. The frequency and waveform of the voltage supplied by the oscillator were measured with a frequency meter F_1 and an oscilloscope O.

Next, a temperature stabilizer ST was switched on. The initial temperature T_0 was set by selecting a suitable current flowing through a heater H in the liquid ^{4}He bath. A digital ammeter DA made it possible to monitor the stabilizer operation. While sound was emitted continuously by the quartz transducer, the angle θ was varied slowly and the resistances of the thermometers T_1 and T_2 were measured with ac bridges S-71 and S-72 and recorded simultaneously with an XY two-pen recorded REC as a function of angle of incidence of the sound. The X input of the recorder received a voltage proportional to the angle θ from the output of a digital-analog converter DAC connected to a frequency meter F_2 that measured the frequency of the LC oscillator. The recorder inputs Y_1 and Y_2 were the voltages supplied by the bridge outputs.

4. RESULTS OF MEASUREMENTS

Gold

The method was tested and the first measurements were carried out on a sample of gold at temperatures 0.05–0.1 °K. The measurements were made without temperature stabilization in the first variant of the system in which the angle could be varied only in one direction away from the normal. The quartz transducer emitted at 20 MHz. Two identical carbon thermometers T_1 and T_2 were used. In view of the negligible specific heat of the sample and thermometers, compared with ^{4}He, and because of their short relaxation times ($\tau \lesssim 10^{-2}$ sec), the thermometers T_1 and T_2 gave synchronously the temperature of the liquid when the quartz transducer was switched off.

In the absence of sound the readings of both thermometers indicated an identical and monotonic rise of the temperature when the sample was rotated at a constant velocity; the rate of rise depended on the rotational velocity and on the initial drift. When an acoustic wave was incident on the sample, the dependence of its temperature on the angle exhibited a peak at $\theta \sim 12.5°$ which amounted to $\Delta T \sim 0.5 \times 10^{-3}$ °K and which was not recorded by the thermometer immersed in liquid helium.

Figure 4 shows two typical records obtained experimentally: a) at $T = 67 \times 10^{-3}$ °K when the angle was varied from 0 to 15°; b) at $T = 68 \times 10^{-3}$ °K when the angle was varied from 6 to 15°. The first record took 1.5 h to obtain. An analysis of the curves indicated that even when the sample was rotated very slowly the temperature of the liquid was constant only within 10^{-4}–10^{-3} °K. In the angular range 0–6° the temperature of the sample followed the temperature of the liquid and began to deviate only at larger angles, reaching a maximum at the angle of ~12.5°, and then falling again.
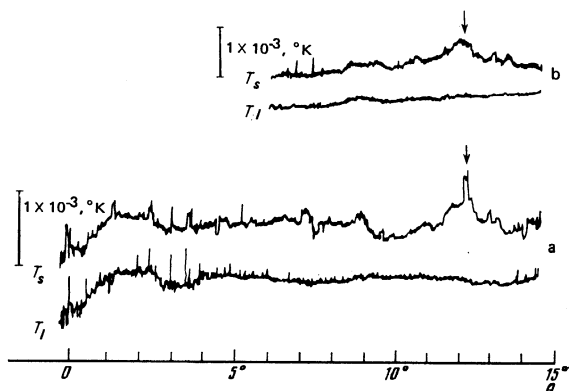
Our experiments on gold thus showed that in the vicin-

FIG. 4. Records of the temperature of a solid sample of gold (T_s) and of the temperature of liquid ^{4}He (T_l) plotted as a function of angle of incidence of sound θ at two bath temperatures T: a) $T = 67 \times 10^{-3}$ °K ($U = 15$ mV); b) $T = 68 \times 10^{-5}$ °K ($U = 20$ mV); U is the voltage across the quartz transducer. The temperature scale is given in the figure. The frequency of sound was $f = 20$ MHz. The time to obtain the records in case a amounted to 1.5 h. The arrows point to the Rayleigh peaks.

ity of an angle close to the critical value ($\theta_2 = 12°12'$) the temperature of the sample was increased by the incident sound and this could be attributed to absorption of Rayleigh waves.

Tungsten

A tungsten single crystal was selected because of its high purity and because the velocity of sound in this material was practically isotropic. Acoustic waves were excited at frequencies of 10 and 30 MHz (fundamental and third harmonic, with the exact values 9.61 and 28.83 MHz). Two identical germanium thermometers were used to measure the temperatures. The angle of incidence of the acoustic waves was varied continuously from −20 to +20°. The temperature stabilizer suppressed the drift and the large temperature fluctuations. The residual fluctuations were recorded simultaneously by the two thermometers in the liquid and at the solid sample. In this way the irregularities on the signal plot could be eliminated by comparing the records of the sample and liquid temperatures.

In the absence of ultrasound the thermometer at the sample reproduced synchronously the temperature of the liquid throughout the angular range. In the presence of ultrasound the temperature of the sample increased by $\Delta T \sim 0.5 \times 10^{-5}$ °K above the temperature of the liquid and this happened only within the range of angles of incidence $\theta = \pm 6°$; outside this range the temperature rise decreased strongly, vanishing for $\theta \geqslant 13°$.

Figures 5 and 6 supplement the results published earlier[5] and they show the acoustically induced rise of the temperature of the sample as a function of the angle of incidence of sound of frequencies 10 and 30 MHz at temperatures 0.2–0.4 °K recorded for various acoustic radiation powers proportional to the square of the effective voltage U^2 applied to the quartz transducer. These figures include also the transmission coefficient of sound $\alpha(\theta) = w(\theta)\cos\theta$ (the difference between α and w

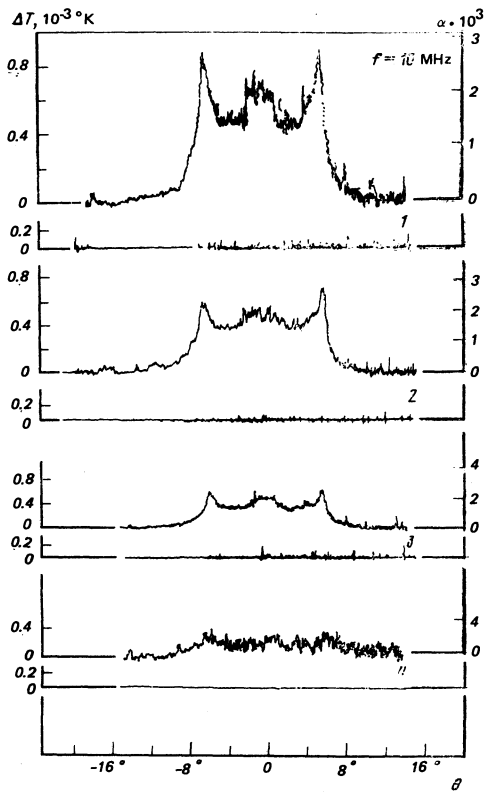FIG. 5. Records of the temperature rise of a sample of tungsten due to the incidence of sound (upper curves) and of the temperature of liquid ^{4}He (lower curves), plotted as a function of the angle of incidence of sound. Bath temperature $T = 0.218\,°K$, frequency of sound $f = 10$ MHz, voltage across quartz transducer: 1) $U = 200$ mV; 2) 210 mV; 3) 155 mV; 4) 83 mV. The scale on the right applies to the transmission coefficient of sound. The time to obtain one record was ~30 min.

FIG. 6. Records of the temperature rise of a sample of tungsten due to the incidence of sound (upper curves) and of the temperature of liquid ^{4}He (lower curves), plotted as a function of the angle θ for different bath temperatures at sound frequency $f = 30$ MHz: 1) $T = 0.218\,°K$, $U = 43$ mV; 2) $T = 0.218\,°K$, $U = 53$ mV; 3) $T = 0.255\,°K$, $U = 70$ mV; 4) $T = 0.321\,°K$, $U = 105$ mV; 5) $T = 0.401\,°K$, $U = 124$ mV.

at the angle of 6° was less than 0.5%, whereas at the angle of 15°, it was ~3%). The value of $\alpha(\theta)$ was calculated from the temperature rise ΔT normalized to zero angle using the following expression for α:

$$\alpha(0) = \frac{4\rho c D c_l}{(\rho c + D c_l)^2} \approx \frac{4\rho c}{D c_l} = 1.4 \cdot 10^{-3}$$

(c_l is the velocity of longitudinal sound in a solid).

Records were taken on different days but without heating the sample. When the sample was heated to liquid-nitrogen temperature (by evaporation of the ^{4}He from the measuring chamber) and the ^{4}He was condensed again, the results were somewhat different: the temperature rise at $\theta = 0$ was less and the Rayleigh peaks decreased. This could be due to contamination of the sample surface by the condensed gases that increased the proportion of the reflected energy.

5. DISCUSSION OF RESULTS

A detailed investigation was made of the transmission of sound across the interface between liquid helium and tungsten.

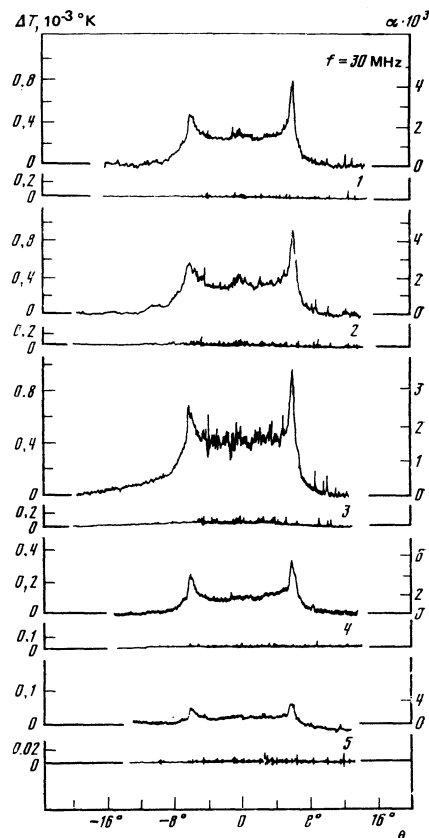The experimental curves (see Figs. 5 and 6 here and also Figs. 1 and 2 in Ref. 1) indicate that acoustic phonons pass from helium into a solid only in a narrow range of angles near normal incidence. In the angular range $\theta > 20_R$ there is no ultrasonically induced increase in the temperature of tungsten (to within $10^{-6}\,°K$) and, consequently, in this range we can assume that phonons are totally reflected by the interface. It is clear from Fig. 1 that the effect is linear; the temperature of the sample rises proportionally to the acoustic power.

At $\theta = \pm 6°$ there are sharp maxima of the temperature rise, which are more pronounced at the sound frequency 30 MHz. The maxima correspond to the Rayleigh angle of incidence (the calculated Rayleigh angle $\theta_R = 5.2°$ agrees with the experimental value within the limits of the measurement error). The observed peaks are similar to the anomalies which appear in the experiments on gold at the angle $\approx 12.5°$. Since these peaks are symmetric relative to the normal at both investigated frequencies at both temperatures, and since they lie within the range of angles of total internal reflection ($\theta > \theta_2 \approx 4.8°$), their appearance may be attributed to an increase in the energy passage resulting from the absorption of Rayleigh surface waves excited resonantly by the incident acoustic wave.

It is worth pointing out two features of the experimental $\alpha(\theta)$ plots. Firstly, at 30 MHz the Rayleigh peaks

at $-\theta_R$ and $+\theta_R$ are of different height, whereas at 10 MHz they are usually equal. This may be due to an inhomogeneous distribution of the intensity across the sound beam, with the inhomogeneity increasing on increase in the attenuation of sound in helium.[22] If the acoustic beam axis does not coincide with the centers of symmetry and with the rotation axis of the sample, the total energy of the acoustic wave incident on the sample is different for $-\theta$ and $+\theta$, and this may be responsible for the different heights of the resonance peaks. The difference increases on increase in the attenuation, i.e., on increase in the frequency.

Secondly, there are small maxima at $\theta = 0$ which appear only at low temperatures ($T \sim 0.2$ °K) and are stronger at 10 MHz. It is clearly due to the amplification of the energy of sound incident on the interface at $\theta = 0$ because of its repeated reflection between the quartz transducer and the sample. The effect increases on reduction in the attenuation in the liquid, i.e., it increases when the temperature is lowered and the frequency is reduced.

We shall compare the experimental results first with the generalized acoustic theory of the passage of a plane acoustic wave through the interface between a liquid and an isotropic solid,[7,12,13] since this theory provides the most general description of the process of reflection and refraction of waves on a boundary between two media. We shall assume that the attenuation in the liquid is zero. We shall allow for the attenuation in the solid by introducing complex wave numbers

$$k_{l,t} = \omega/c_{l,t} = k_{l,t}^{(0)}(1 + ip_{l,t})$$

or complex velocities $c_{l,t} = c_{l,t}^{(0)}(1 + ip_{l,t})^{-1}$, where $k_{l,t}^{(0)}$ and $c_{l,t}^{(0)}$ are the real wave numbers and velocities. The attenuation parameters $p_{l,t}$ can be expressed in terms of the sound energy absorption coefficients:

$$p_{l,t} = \gamma_{l,t} c_{l,t}^{(0)}/2\omega = \lambda_{l,t}/4\pi l_{l,t},$$

where $\gamma_{l,t}$ is the absorption coefficient (neper per unit length), $\lambda_{l,t}$ is the sound wavelength, and $l_{l,t}$ is the characteristic energy attenuation length. Moreover, to satisfy the boundary conditions we have to generalize the Snell law to the case of complex wave numbers.

Then, the transmission coefficient of the acoustic energy is

$$w(\theta) = 4\mathrm{Re}\,(\beta)/|\beta+1|^2, \tag{5}$$

where

$$\beta = \frac{D}{\rho}\cos\theta\left\{\frac{c_t}{c}\left[1 - 2\left(\frac{c_t}{c}\sin\theta\right)^2\right]^2\left[1 - \left(\frac{c_t}{c}\sin\theta\right)^2\right]^{-1/2} + 4\left(\frac{c_t}{c}\right)^3\sin^2\theta \times \left[1 - \left(\frac{c_t}{c}\sin\theta\right)^2\right]^{1/2}\right\}. \tag{6}$$

It follows from Eqs. (5) and (6) that the coefficient of transmission of sound from the liquid to the solid is governed by the following parameters of these media: $\rho, D, c, c_l, c_t, p_l, p_t$.

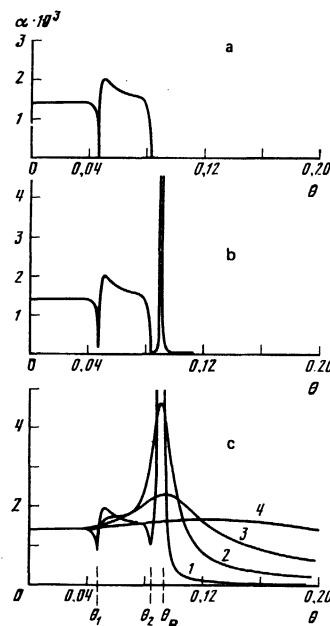Figure 7 shows the plots of $\alpha(\theta) = w(\theta)\cos\theta$ computer-

FIG. 7. Calculated dependences of the energy transmission coefficient of a plane monochromatic acoustic wave on the angle of incidence on the interface between ^{4}He and tungsten obtained for different attenuation parameters p of sound in tungsten: a) $p=0$; b) $p=3\times10^{-4}$; c1) $p=10^{-2}$; c2) $p=10^{-1}$; c3) $p=0.3$; c4) $p=1$.

calculated by applying the above formulas to an interface between liquid ^{4}He and tungsten at some fixed values of $p = p_l = p_t$. The following numerical parameters were assumed in these calculations: $\rho = 0.145$ g/cm^3, $D = 19.4$ g/cm^3, $c = 2.4\times10^4$ cm/sec, $c_l = 5.11\times10^5$ cm/sec, $c_t = 2.88\times10^5$ cm/sec. It is clear from these curves that there are three critical angles of incidence: $\theta_1 = 0.047$, $\theta_2 = 0.083$, and $\theta_R = 0.09049$, at which $\alpha(\theta)$ have singularities. The angles θ_1 and θ_2 are governed by the Snell law, when the sines of the angles of refraction of the longitudinal and transverse waves in the solid become unity. Then, in the absence of attenuation [$p = 0$, Fig. 7(a)], total internal reflection ($\alpha = 0$) is observed at $\theta = \theta_1$ and at $\theta = \theta_2$. There is no Rayleigh peak at $p = 0$. Naturally, in this case Rayleigh waves may be created on the metal surface but they transmit their energy only to the liquid.[23,24]

In the presence of absorption in the solid ($p > 0$), the $\alpha(\theta)$ curve acquires a Rayleigh peak whose height and width depend on p. This is due to the fact that the attenuation coefficient of a Rayleigh wave traveling in a surface layer of thicknesses of the order of λ is governed by the attenuation coefficients of bulk waves, mainly the attenuation of the transverse wave.[24]

Figure 7(b) shows the dependence $\alpha(\theta)$ for $p = p_l = p_t = 3\times10^{-4}$. (This value of p corresponds to the absorption coefficients of ultrasound of tungsten amounting to $\gamma_l = 1$ dB/cm and $\gamma_t = 1.7$ dB/cm obtained at 30 MHz from the measurements reported in Refs. 25 and 26.) The height of the Rayleigh peak in this figure is $\alpha_R = \alpha(\theta_R) \doteq 0.74$ and the width at midheight is $\delta = 7.55 \times10^{-5}$ rad $= 15''$; the minimal values of α at the angles θ_1 and θ_2 are no longer equal to zero. Figure 7(c)
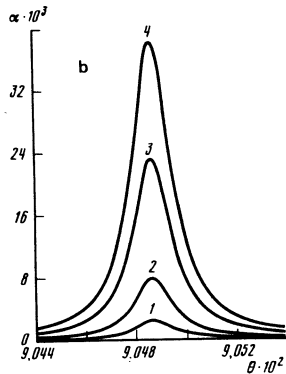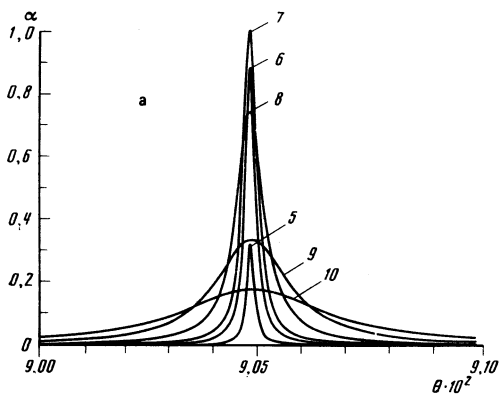
FIG. 8. Calculated dependences of the energy transmission coefficient of a plane monochromatic acoustic wave on the angle angle of incidence of sound on the interface between ^{4}He and tungsten in the vicinity of the Rayleigh peak obtained for different attenuation parameters p: 1) 6×10^{-8}; 2) 2×10^{-7}; 3) 6×10^{-7}; 4) 10^{-6}; 5) 10^{-5}; 6) 5×10^{-5}; 7) 10^{-4}; 8) 3×10^{-4}; 9) 10^{-3}; 10) 1.9×10^{-3}.

shows the plots of $\alpha(\theta)$ for high values of p.

It is clear from Fig. 7 that in the presence of absorption of sound in a solid there is a considerable change in the nature of the curves for the angles $\theta > \theta_2$, whereas in the range $\theta < \theta_2$ the change in α is not so large.

Figure 8 illustrates the process of appearance of the Rayleigh peaks, beginning from negligible but finite attenuations $p \neq 0$. It is clear from this figure that the peaks are typical of resonance curves whose parameters (width and height) are determined by attenuation. The total transmission at the Rayleigh angle $[w(\theta_R) = 1$ and $\alpha(\theta_R) \approx 1]$ in the liquid ^{4}He–tungsten system occurs at $p = 10^{-4}$ (curve 7). For lower values of p the amplitude and the area under the Rayleigh peak decrease rapidly, but in the range $p > 10^{-4}$ the amplitude decreases whereas the area increases. At very high values of p the $\alpha(\theta)$ dependences are no longer of the resonance type [Fig. 7(c)].

At very low values of p $[<10^{-6}$, curves 1–4 in Fig. 8(b)] the amplitude of α_R rises linearly on increase in p, whereas the peak width is approximately constant and equal to $\delta_0 = 1.8 \times 10^{-6} = 4''$.

The calculated integral of the transmitted energy of a plane wave

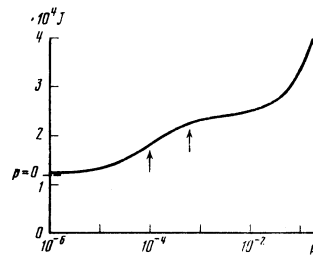$$J = \int_0^{\pi/2} \alpha(\theta)\, d\theta \qquad (7)$$

FIG. 9. Calculated dependence of the integral of the transmitted acoustic energy J, given by Eq. (7), on the attenuation parameter p. The arrows identify the limits of variation in the integrals of the experimental curves $\alpha(\theta)$ and the corresponding values of p.

is plotted in Fig. 9 as a function of p. Here, the dashed line on the ordinate represents the energy transmitted into a solid only in the form of longitudinal and transverse waves incident at a subcritical angle $(p = 0)$. An increase in the attenuation increases the total energy integral and the point of inflection of the curve (corresponding to the maximum of its derivative) occurs at $p \approx 10^{-4}$, when the transmission coefficient α at the Rayleigh angle is equal to unity.

It is clear from Fig. 9 that if we ignore the very large and very small values of p, we find that the contribution of the surface waves is approximately equal to the contribution of the bulk waves. A considerable increase in the integral is observed at $p \approx 1$. However, when this strong attenuation takes place, the process is no longer of the wave type. In the case of very weak attenuation $(p < 10^{-6})$ the Rayleigh wave contribution is small, representing only a few percent of the contribution of the bulk waves.

The following difficulty was encountered in comparing the experimental and calculated curves. It was not possible to fit the height and width of the calculated curves to the Rayleigh peaks. The value of p which agrees with the width of the peaks is $(3.6-4) \times 10^{-2}$, whereas the height of the calculated peaks is then $(10-12) \times 10^{-3}$, i.e., it is 2.5 times greater than the experimental value. The heights of the peaks can be matched by selecting p to be $(9-10) \times 10^{-2}$, but then the width of the calculated peaks is twice as large as the experimental value.

The main reason why calculations cannot be used to fit the experimental results is that for all these values of p the theoretical peaks have extensive tails that contribute 11–12 and 28–30% to the integral of the transmitted energy beyond the angle $\theta = 0.2$. The experimental curves make zero contribution beyond the angle 0.15, which suggests that the value of p is smaller.

However, the theoretical curves are calculated for an infinite plane interface and an ideal plane wave. The first condition means that the size of the sample should not be less than the characteristic length l. In our experiments this condition was satisfied approximately only at $f = 30$ MHz. The second condition cannot be met even in principle because of the real broadening of the acoustic beam. The quartz transducer used in our experiments was characterized by an acoustic beam divergence close to the diffraction limit in water and tolu-

TABLE I. Principal parameters of experimental curves.

f, MHz	T, °K	U, mV	$\alpha_R \cdot 10^3$	$\delta \cdot 10^3$, rad.	$10^4 J$	$10^4 p$
10	0.218	200	2.67		1.87	1.25
10	0.28	200	2.41		1.8	1.0
30	0.21	43	4.5	7.2	2.05	2.4
30	0.218	53	4.36	8.6	2.02	2.2
30	0.218	53	4.2	9.2	2.02	2.2
60	0.258	70	4.7	9.2	2.1	3.0
30	0.311	80	4.5	10.5	2.25	6.6
30	0.321	105	4.37	11.8	2.22	5.8
30	0.401	124	2.8	11.8	2.06	2.5

Note. Here, f is the frequency of the incident sound, T is the temperature of the helium bath, α_R is the energy transmission coefficient for an acoustic wave incident at the Rayleigh angle, U is the effective voltage across the piezoelectric quartz transducer, δ is the width of the Rayleigh peak at midheight, $J = \int_0^{\theta_2} \alpha(\theta) d(\theta)$ is the integral of the experimental curve plotted as a function of the angle of incidence, and p is the attentuation parameter calculated by comparing the experimental and theoretical values of the integral.
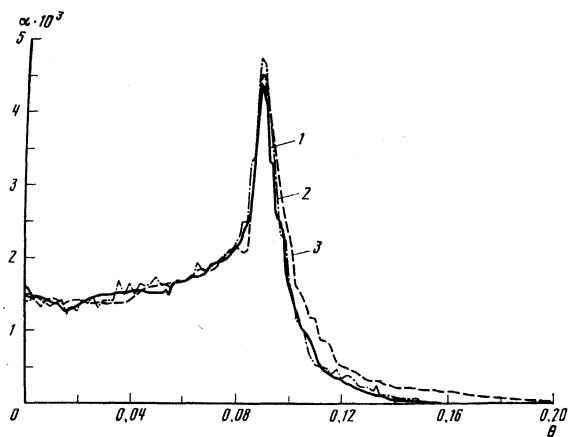

FIG. 10. Normalized experimental $\alpha(\theta)$ curves for sound frequency $f = 30$ MHz at three temperatures: 1) $T = 0.21$ °K; 2) $T = 0.258$ °K; 3) $T = 0.311$ °K (Ref. 1).

ene. The expected diffraction broadening of the beam in helium at 10 and 30 MHz is 6' and 2'. However, the experimental curves (Fig. 6) and Table I indicate that the smallest width of a Rayleigh peak at $T = 0.218$ °K and $f = 30$ MHz is about 25', which is an order of magnitude greater than the diffraction limit. This may be due to the broadening of the acoustic beam because of imperfections of the transducer and because of the roughness of the surface of the sample. A simple calculation shows that in the case of a smooth but wave-like surface of the sample (such a surface may be formed by electropolishing) with a period of ~330 μ and a height of ~0.3 μ the range of incidence angles and, consequently, the Rayleigh peak broaden to 25'.

The angular distribution of the intensity of the incident wave and broadening of the range of the incidence angles result in smoothing out of all the features of the experimental curve $\alpha(\theta)$ and in broadening of the Rayleigh peak by an amount $\Delta\theta \gg \delta$. An additional broadening (in excess of 25') on increase in temperature may be due to an increase in the attenuation of sound in helium.[22]

If the wavy surface of the sample does not alter the transmission coefficient of sound (when the period of the surface irregularity is $>\lambda$, Ref. 27), the area under the Rayleigh peak as well as the area under the whole experimental curve $\alpha(\theta)$ are the same as in the ideal case. Thus, if we use the constancy of the energy integral, we can compare the experimental results with the theory and estimate the attenuation parameter p (and γ) for a given sample.

With this in mind we normalized the experimental curves as shown in Fig. 10 (i.e., until the best agreement with the curves in the subcritical region was obtained) and this was done by comparing the integrals

$$J(\theta) = \int_0^\theta \alpha(\theta) d(\theta) \tag{8}$$

of the experimental and theoretical $\alpha(\theta)$ curves, selecting such a value of p for each integral of the experimental curve (experimental integral) that the calculated in-

tegral agreed best with the experimental value. Typical dependences of the integral of the energy transmitted into a sample on the angle of incidence are plotted in Figs. 11 and 12 for different temperatures and acoustic frequencies.

The attenuation parameter $p = (2-6) \times 10^{-4}$ found in this way for tungsten at $f = 30$ MHz (Table I) is in satisfactory agreement with the experimentally determined bulk absorption of sound represented by $p = 3 \times 10^{-4}$ (Refs. 25 and 26). The experimental integral of the total energy is then about twice the integral for the critical angle θ_2, i.e., the contribution of the energy of surface waves is approximately equal to the contribution of the bulk waves.

The attenuation parameter for sound of frequency 10 MHz is $p = (1.0-1.25) \times 10^{-4}$. It should be pointed out that although the precision of the determination of the energy integral from the experimental $\alpha(\theta)$ curves is 5-10%, a comparison of the experimental and calculated integrals gives only an estimate of the parameter p which is subject to an error of the same order of magnitude as the value itself (50-100%), because—as pointed out above—the experimental conditions do not agree fully with those assumed in the calculations (the sample is bounded, the surface is rough, and sound is
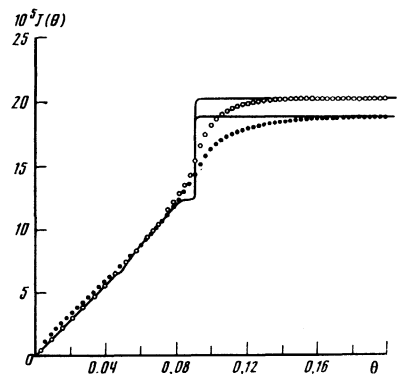

FIG. 11. Integral of the transmitted acoustic energy, given by Eq. (8), plotted as a function of the angle θ for the experimental (points) and theoretical (continuous curves) dependences $\alpha(\theta)$: 1) $f = 30$ MHz; 2) $f = 10$ MHz; $T = 0.218$ °K.
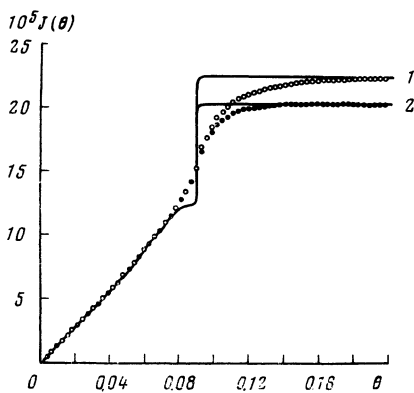
FIG. 12. Integral of the transmitted acoustic energy, given by Eq. (8), plotted as a function of the angle θ for the experimental (points) and theoretical (continuous curves) dependences $\alpha(\theta)$: 1) $T = 0.311\,°K$; 2) $T = 0.218\,°K$; $f = 30$ MHz.

attenuated in helium).

Thus, in the case of an unbounded tungsten sample with a flat surface the dependence of the transmission coefficient of sound across the interface with liquid helium on the angle of incidence of an ideal plane wave of frequency 30 MHz should have the form shown in Fig. 7(b). At $f = 10$ MHz the dependence is similar but in this case we have $\alpha(\theta_R) = 1$ and $\delta = 3.7 \times 10^{-5} = 8''$. The case shown in Fig. 7(a) can in practice be observed at low frequencies $f \ll 10$ MHz.

The $\alpha(\theta)$ curves of type designated 1 and 2 in Fig. 7(b) can clearly be expected at high frequencies (thermal phonons) even in the presence of defects in the surface layer. In the case of curves 3 and 4 in Fig. 7(c) a sample should have on the surface a sound-absorbing layer of thickness comparable with the wavelength of sound, which is possible in the case of thermal phonons at $T > 1\,°K$.

It is clear from Table I that at $f = 30$ MHz the energy integral, and consequently the attenuation parameter p, increases with increase in temperature, which—according to the theory—might indicate an increase in the attenuation in the solid when temperature is increased if the attenuation in the liquid were to remain negligible. However, the acoustic attenuation parameter of ^{4}He increases with temperature like T^4 (Ref. 28), and at 30 MHz it becomes comparable with the attenuation in a solid at $T \sim 0.4\,°K$. In this case the energy transmission associated with the absorption of Rayleigh waves may be due to the attenuation in the solid or in the liquid. The above theoretical calculation then becomes incomplete and it has to be refined to allow for the case when the attenuation in the liquid can no longer be ignored.

It is interesting to compare the experimental results with the calculations carried out using the generalized classical formulas with the theory of Andreev.[2] Andreev allowed for the absorption of the energy of an acoustic wave by conduction electrons through introduction of an additional term Y in the classical formula for the reflection coefficient.[7] This term represents the impedance for the transmission, across a boundary, of sound accompanied by the excitation of a Rayleigh wave,

and it has a real part in the vicinity of the Rayleigh angle of incidence. Andreev gives the following expression for $w(\theta)$ in the vicinity of θ_R (it is assumed that $l_e/\lambda \gg 1$, where l_e is the mean free path of the electrons):

$$w(\theta) = \frac{4B}{(B+1)^2 + (\theta - \theta_R)^2 (HDc_t^2/\rho c^2)^2},\qquad(9)$$

where

$$B = \frac{Y}{\rho c} = \frac{p_0^4}{(\pi \hbar)^3}\frac{G}{\rho c},$$

H and G are functions of the elastic constants of helium and the metal (in the case of tungsten we have $G = 0.07$), and p_0 is the electron momentum on the Fermi surface.

We shall now compare the Andreev results with calculations carried out using the generalized acoustic formula. With this in mind we consider Eq. (5) for $w(\theta)$ in the vicinity of the Rayleigh angle θ_R and we assume that the attenuation parameter is small, $p \ll 1$. We shall expand $w(\theta)$ in powers of p and $\theta - \theta_R$, and shall ignore terms of the second order of smallness:

$$w(\theta) = \frac{4pE}{(pE+1)^2 + (\theta - \theta_p)^2 M^2};\qquad(10)$$

here E and M are functions of the elastic constants and of the ratio of the densities of helium and metal (without allowance for the attenuation).

We can readily see that Eqs. (9) and (10) are similar and that they describe a resonance curve if $B = pE$ and $HDc_t^2/\rho c^2 = M$. In the range of very weak absorptions ($pE \ll 1$ and $B \ll 1$), both formulas give for a Rayleigh peak the same width $\delta = 1.8 \times 10^{-5}$ (which is independent of the attenuation)—see curves 1–4 in Fig. 8—and the height of the peak α_R is in both cases proportional to the absorption of sound [p in Eq. (10) and p_0^4 in Eq. (9)]. Hence, it follows that the theory of Andreev predicts the same resonance of the transmission of energy in the vicinity of the Rayleigh angle as does the generalized acoustic theory.

An approximate calculation for tungsten gives $B \approx 10^{-2}$ (if we assume that $p_0 = 2\hbar/a$, where a is the lattice constant), and hence we find that $\alpha_R \approx 4 \times 10^{-2}$ and $\delta = 1.84 \times 10^{-5}$. These are the parameters that a Rayleigh peak should have for $p \approx 10^{-6}$, which is two orders of magnitude less than the experimental value. However, Jones and Rayne pointed out some time ago[26] that the measured absorption of ultrasound in tungsten (and molybdenum) is two orders of magnitude higher than that calculated from the theory of free electrons. In some papers (see, for example, Ref. 29) it has been mentioned that the Fermi surface of transition metals is far from that expected in the model of free electrons, and the absorption of ultrasound is then best described by the tight-binding approximation. This approximation has been used to calculate the absorption of sound in tungsten by electrons and holes allowing for the deformation potential.[25] The absorption coefficients calculated by this method are in satisfactory agreement with our experimental results.

Recently Urazakov and Fal'kovskii[30] showed that a sharp peak of the transmission coefficient of sound incident at angles outside the critical range can also be

due to the scattering of Rayleigh waves by the surface irregularities, accompanied by their transformation into bulk waves. The effect is analogous to the scattering by periodic irregularities, right-angled corners, and steps with a rounding radius $r < \lambda$ (Refs. 27, 24, and 31). The peak profile should then depend on the impedances of the media and on the parameters of the irregularities. An investigation of this mechanism would require separate study because in the present investigation the dependence of the shape of a Rayleigh peak on the nature of surface irregularities has not been specifically investigated.

CONCLUSIONS

We have thus established experimentally that sound incident from liquid helium on the surface of a metal crosses the interface between them only in a limited range of angles of incidence, which does not exceed twice the Rayleigh angle in the case of tungsten.

The angular dependence of the energy transmission coefficient in the range beyond the critical angle of incidence has a sharp maximum due to the absorption of Rayleigh waves in the metal.

It is shown that the Rayleigh waves make an approximately the same contribution as bulk waves (at subcritical angles) to the energy flux across the interface.

The transmission of the sound energy across an interface can be described satisfactorily by the generalized acoustic theory allowing for the attenuation of bulk waves in a solid.

It has been shown that the generalized acoustic theory and the theory of Andreev are equivalent in their description of the transmission of sound in the vicinity of the Rayleigh angle.

The absorption of the energy of Rayleigh waves is governed by the absorption coefficient of bulk ultrasonic waves. The absorption coefficients of tungsten are in quantitative agreement with the published experimental data and with the theoretical values calculated on the assumption of the electron absorption mechanism.

[1])The oscillator circuit was suggested by V. I. Voronin.

[1]K. N. Zinov'eva, Pis'ma Zh. Eksp. Teor. Fiz. 28, 294 (1978) [JETP Lett. 28, 269 (1978)].

[2]A. F. Andreev, Zh. Eksp. Teor. Fiz. 43, 358, 1535 (1962) [Sov. Phys. JETP 16, 257, 1084 (1963)]; Kandidatskaya dissertatsiya (Thesis for Candidate's Degree), Institute of Physics Problems, Academy of Sciences of the USSR, Moscow, 1964.

[3]P. L. Kapitza, Zh. Eksp. Teor. Fiz. 11, 1 (1941).

[4]I. M. Khalatnikov, Zh. Eksp. Teor. Fiz. 22, 687 (1952).

[5]I. M. Khalatnikov, Vvedenie v teoriyu sverkhtekuchesti, Nauka, M., 1965 (An Introduction to the Theory of Superfluidity, Benjamin, New York, 1965); Teoriya sverkhtekuchesti (Theory of Superfluidity), Nauka, M., 1971.

[6]W. A. Little, Can. J. Phys. 37, 334 (1959).

[7]L. M. Brekhovskikh, Volny v sloistykh sredakh (Waves in Layered Media, 2nd ed.), Nauka, M., 1973.

[8]J. Weber, W. Sandmann, W. Dietsche, and H. Kinder, Phys. Rev. Lett. 40, 1469 (1978).

[9]I. M. Kahlatnikov and I. N. Adamenko, Zh. Eksp. Teor. Fiz. 63, 745 (1972) [Sov. Phys. JETP 36, 391 (1973)].

[10]W. A. Little, Phys. Rev. 123, 435 (1961).

[11]L. D. Landau and E. M. Lifshitz, Teoriya uprugosti, Nauka, M., 1965, p. 143 (Theory of Elasticity, 2nd ed., Pergamon Press, Oxford, 1970).

[12]H. Haug and K. Weiss, Phys. Lett. A 40, 19 (1972).

[13]R. E. Peterson and A. C. Anderson, J. Low Temp. Phys. 11, 639 (1973).

[14]N. G. Mills, A. F. G. Wyatt, and R. A. Sherlock, J. Phys. C 8, 289 (1975); R. A. Sherlock, N. G. Mills, and A. F. G. Wyatt, J. Phys. C 8, 300 (1975).

[15]A. F. G. Wyatt, G. J. Page, and R. A. Sherlock, Phys. Rev. Lett. 36, 1184 (1976).

[16]V. M. Merkulova, Akust. Zh. 15, 464 (1969) [Sov. Phys. Acoust. 15, 404 (1970)].

[17]F. L. Becker and R. L. Richardson, in: Research Techniques in Nondestructive Testing (ed. by R. S. Sharpe), Vol. 1, Academic Press, New York, 1970, p. 91.

[18]R. Truell, C. Elbaum, and B. B. Check, Ultrasonic Methods in Solid State Physics, Academic Press, New York, 1969 (Russ. Transl., Mir, M., 1972, p. 227).

[19]K. N. Zinov'eva and G. É. Karstens, Prib. Tekh. Eksp. No. 2, 249 (1974).

[20]S. T. Boldyrev, K. N. Zinov'eva, F. M. Vorobkalo, L. I. Zarubin, and I. Yu. Nemish, Materialy 20-go Vsesoyuznogo soveshchaniya po fizike nizkikh temperatur, NT-20 (Proc. Twentieth All-Union Conf. on Physics of Low Temperatures, NT-20), Chernogolovka, 1978, p. 277.

[21]V. I. Voronin, Prib. Tekh. Eksp. (in press).

[22]B. K. Laĭkhtman and A. V. Lomakin, Pis'ma Zh. Eksp. Teor. Fiz. 23, 624 (1976) [JETP Lett. 23, 572 (1976)].

[23]A. Schoch, Ergeb. Exakten Naturwiss. 23, 127 (1950).

[24]I. A. Viktorov, Fizicheskie osnovy primeneniya ul'trazvukovykh voln Réleya i Lémba v tekhnike, Nauka, M., 1966 (Rayleigh and Lamb Waves, Plenum Press, New York, 1967).

[25]K. B. Vlasov, A. B. Rinkevich, and R. Sh. Nasyrov, Fiz. Met. Metalloved. 47, 524 (1979).

[26]C. K. Jones and J. A. Rayne, Phys. Lett. 13, 282 (1964).

[27]L. M. Brekhovskikh, Akust. Zh. 5, 282 (1959) [Sov. Phys. Acoust. 5, 288 (1959)].

[28]B. M. Abraham, Y. Eckstein, J. B. Ketterson, M. Kuchnir, and J. Vignos, Phys. Rev. 181, 347 (1969).

[29]D. P. Almond and J. A. Rayne, J. Low Temp. Phys. 23, 7 (1976).

[30]E. I. Urazakov and L. A. Fal'kovskiĭ, Zh. Eksp. Teor. Fiz. 79, 261 (1980) [Sov. Phys. JETP 52, 132 (1980)].

[31]G. W. Farnell, "Types and properties of surface waves," in: Acoustic Surface Waves (ed. by A. A. Oliner), Springer-Verlag, Berlin (1978), p. 13 [Topics in Applied Physics, Vol. 24].

Translated by A. Tybulewicz